Structural Analysis of NGC 2371-2 Using Deep Images in [O-III] and Tri-color

Erin O. Martin

A senior thesis submitted to the Carthage College Physics Department
in partial fulfillment of the requirements for the Bachelor of Arts Degree in Physics

Carthage College
Kenosha, WI

May 20, 2009

Abstract

The odd structure of NGC 2371/2, a planetary nebula (PN) has been studied. This nebula has ejected gas during the final stages of stellar evolution. These gases do not appear to be symmetric as would be expected. Using a narrow-band [O-III] filter centered at 5007 Angstroms ($\mathring{A}$) with the Steward Observatory 61 inch Kuiper telescope and Mont4K camera, deep field images were obtained to study the faint structure of the PN which have never been studied before. Multiple images were taken and combined to create a final processed image. The total exposure time with an [O III] filter was 9 hours. Using the same instrumentation, 1 hour of exposures were taken with three filters, R, V, and B. These images have been processed and stacked for a final tricolor image. The final [O III] image was contoured under six ranging intensity levels. Each contour ranges in pixel counts by 5,000. This gives detail of the nebula for each intensity level. The final contour plot shows all the contour plots stacked on top of each other. The contours were done in Iraf. The structure of the nebula has been compared to prior studies. These studies show only part of the nebula and miss some of the fainter details that are seen in this paper. In early work the outer gas shell appears to be detached from the nebula; however, through this research the outer shell has faint gas connecting it with the rest of the nebula. Also found in this study were two jets moving NE and SW from the central star.

I Introduction

1.1 Discovery of Planetary Nebulae

Before the time of catalogues, faint fuzzy objects were known as nebulae. When William Herschel began his own observations he divided his findings into eight categories, one of them being Planetary Nebulae (PNe). He called these objects PNe because they are small objects that are well defined and their greenish color reminded him of the planet Uranus, which he had discovered in 1781. These objects were not well understood and were even believed to be faint star clusters. It was not until the discovery of NGC 1514 in November 1790 that it became clear that the star and the gas surrounding it were not superimposed, but part of the same object.

1.2 Stellar Evolution

Stars that reside within the Chandrasekhar Limit, 1.2 through 2.5 solar masses reside on the main sequence of the Hertzsrung-Russll (H-R) Diagram for approximately 10 billion years [1]. After this period, these stars become unstable and go through a fluctuation period. During this time a star moves to the instability strip on the H-R Diagram as seen in Fig. 1 [1].

As these low mass stars become unstable, they go through the red giant stage twice in their lifetime. The first time a star goes through this phase, it stabilizes, as it begins to fuse the inert helium in its core into both carbon and oxygen. It then becomes unstable once again and goes through the red giant stage for the second time. If they were more massive, the carbon-oxygen core could fuse into heavier elements to once again stabilize the star. This would result in a core of neon,

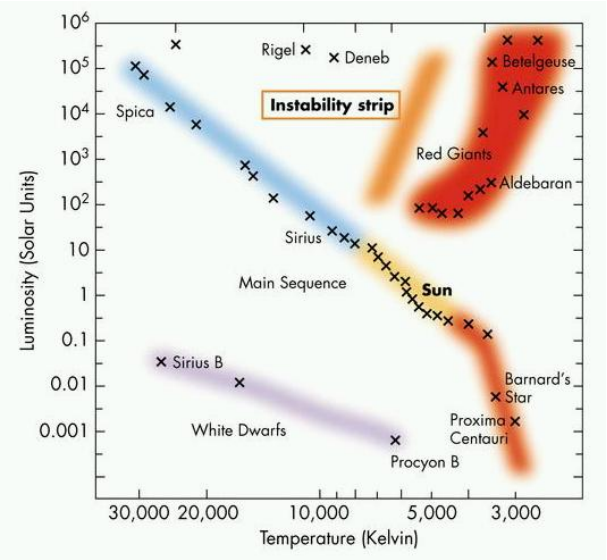

Figure 1: Hertzsrung-Russll Diagram [1]

magnesium, and oxygen. However, this nuclear burning would need the core to be compressed even further than the helium core, which is not possible for low mass stars. At this stage, the star begins to lose its exterior hydrogen envelope through stellar winds [2]. When this mass loss becomes significantly high, the core is believed to reach the Eddington luminosity. The Eddington luminosity is the limit at which an optically thin medium can be accelerated to be removed from an atmosphere against the force of gravity. The Equation for the Eddington luminosity can be found in Eq 1.

$$L_{EDD} = \frac{4\pi GM}{k_e} \qquad Eq.1$$

Where G = $6.67x10^{-11}m^3kg^{-1}s^{-2}$, M is the mass of the star and k_e is the opacity [3].

Radiation pressure destabilizes the atmosphere, and if both the luminosity and opacity are high enough, nothing can stop the materials from surpassing the escape velocity [3]. At the point of the Eddington lumi-

nosity the star undergoes extensive mass loss until helium shell burning can no longer take place. After this, cooling sets in. This causes the star to contract, which increases the effective surface temperature [3]. Under this process the central core of the star will then as a carbon-oxygen core, held stable under the gravitational pressure by electron degeneracy pressure [2]. The WD is surrounded by a hot gas ejected from the star; this is known as a planetary nebula. The hot gas now surrounding the central core of the star was once the star's fuel. This phase of a star lasts for about 10,000 years [1]. These gases would be expected to be a uniform shell of gas; however, this is not the case. Many of these PNe have abnormal structures.

1.3 Structure and Classification of Planetary Nebulae

A single model of all PNe is not possible. The atmosphere of a star can be determined by a few parameters, such as temperature, gravitation and in some cases chemical composition. A star, being a uniform ball of gas, would be expected to produce a uniform shell of gas at the end of its lifetime. However, there are many more parameters that would affect the shape of a PN. There are no two PN that look exactly the same. There are many nebulae with a ring-like structure; still, they do not precisely look the same. Within these irregularities, it is still possible to find reoccurring structure [6].

There are three classifications of different PNe. Class I is known as the planetoid nebulae. This class has only one gaseous envelope with a uniform brightness distribution. Class II PNe have a double-envelope of gas which could signify a relationship to the Class I PNe. Class III is a ring like nebula. The surrounding gas is most prominent along the outer edge of the nebula and there is no sign of a second envelope. The three classes can be seen in Fig. 3. They can also provide an evolutionary indication. Class I are the smallest nebula and increase in size through each class [6].

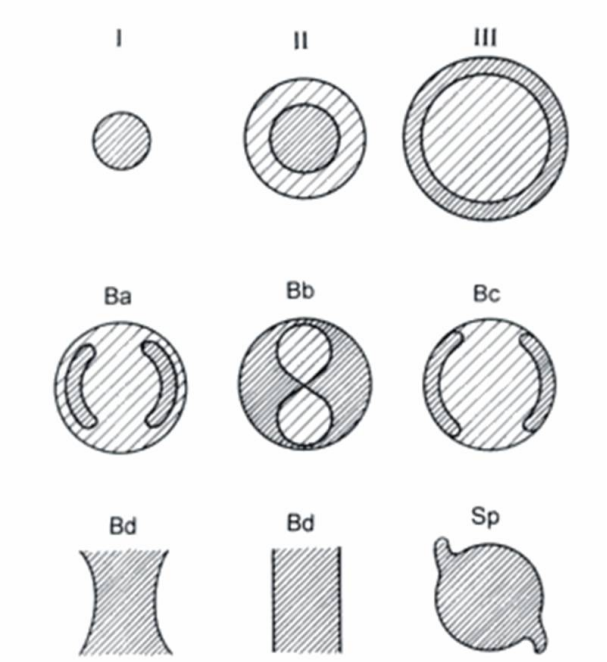

Figure 2: Planetary Nebulae Classes [6]

Within the three classes there is also the possibility of bipolar subclasses. It is possible for all three classes to have a bipolar structure labeled with a B in Fig. 3. There are also different degrees of bipolarity within a class. These are labeled a through d of the increasing development of a bipolar nebula. As a basic standard for bipolarity, a brightness ratio can be taken at the major and minor edges of the nebula. An object is considered to be bipolar when the minor axis is one and a half times brighter than the major axis, this would fall under the first category. In the

next group, the brightness differences are so great that the nebula appears divided into two parts. PNe with this degree of bipolarity often appear to have knots near the edges of the short axis, which are also symmetric with the central star. In the third group, the knots are more developed and almost isolated from the rest of the nebula. The fourth and final group is the most extreme case of bipolarity. They are often known as the rectangular or hourglass objects. They are compressed mostly at the minor axis and elongated at the major axis [6].

Another subclass of PNe is the spiral class denoted Sp. These nebulae appear to have spiral-like arms similar in appearance to spiral galaxies. These arms are believed to be caused both the intrinsic magnetic field of the PNe and the magnetic field of the galaxy. Examples of these different subtypes of PN can be found in Fig. 3 [6].

1.4 Bipolarity and Magnetic Fields

The bipolar structure of PNe is one of the most common structures of these objects. They are often seen with two regions of similar brightness and are symmetric with relation to the central star. There have not been any discoveries of PNe with an odd number of these brighter regions. The binary structure in PNe gives rise to evidence of an electromagnetic influence [6].

The magnetic field of the Milky Way Galaxy has been considered to be a cause of the redistribution of ionized nebular matter. This would cause clumping or grouping of the gas within the nebula, giving it an odd shape. If this is true, a correlation between the directions of the magnetic field lines of the galaxy and the direction of the major axis of a bipolar PN could be determined. However, no such correlation has been found. There seems to be an equal number of PNe with their major axes parallel to the galactic equator as there are perpendicular. Also, bipolar nebulae are often found at higher galactic latitudes where the magnetic field of the galaxy would be too weak to have an influence on the structure [6].

The magnetic field of the WD would also not affect the ionized gases of the nebula. The magnetic field produced from the central star is a dipole and decreases in strength as the cube of the distance. Assuming that the strength of the field is 10^6 gauss at the surface of the WD, it would be close to 10^{-10} gauss at the bright knots in the nebula. This magnetic field strength would not be strong enough to have an effect on the shape of the nebulae [6].

Although both the Galactic and central star's magnetic field do not seem to have an effect on the nebulae, the theory that an electromagnetic field still remained a possibility. This would mean that there must be a magnetic field within the nebulae. The magnetic field of a PN cannot be constant. If it were a constant the gases would not create 'knots' or clumps within the nebula and they would not have bipolarity. The bipolar structure indicates that the magnetic field should vary distinctly, in strength and direction, from one point to another. Also, the field must be symmetric with respect to the axis of the nebula [6]. If PNe are affected by a magnetic field then the clumps of gas should be seen as being of equal brightness and symmetric.

1.5 Nebulae Spectrum

White Dwarf stars are between 1.2 and

2.5 solar masses and approximately the size of Earth. The central pressure inside these objects is about

$$3.8 \times 10^{22} N/m^2.$$

This pressure is estimated to be about 1.5 million times larger than the pressure inside the sun. Thus the surface temperature of a WD is extremely high [4]. The coolest of these stars is near 25,000 K [5]. The gases surrounding these stars are also heated from the central star. When astronomers first began to use a spectrograph on these objects they noticed reoccurring emission lines, which they referred to as "nebulium" lines. Throughout all observations of planetary nebulae, these were the strongest emission lines, as seen in Fig. 3 [6].

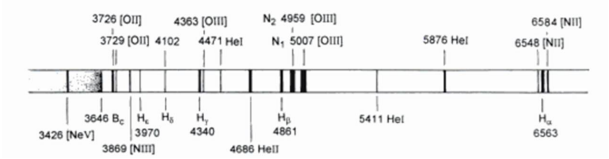

Figure 3: Planetary Nebulae Spectrum [6]

These spectral lines were unknown because nothing before had ever been seen like this. They became known as the forbidden lines because the conditions can not be reproduced on Earth. These lines were denoted $N_1$and N_2, at wavelengths of 5007 $\mathring{A}$ and 4959 $\mathring{A}$. The N was for nebulium, the new element they believed to have discovered. However, a new element was not found. The WD at the center of the nebula provides enough energy to ionize the gaseous materials surrounding it. The strong emission lines that were being observed were that of doubly ionized oxygen or [O III]. The brackets around the O III signify that these are forbidden lines in the laboratory [6]. Planetary Nebulae are often imaged with [O III] filters because most of their light is given off in [O III], or the green end of the spectrum. However, it can also be useful to do tri-color imaging. Looking at the spectrum in Fig. 3 there are strong emission lines in both the red and blue end of the spectrum not just the green. Using three filters a true color image can be made to show greater detail of the nebula.

1.6 NGC 2371-2

The New General Catalogue (NGC) was published in 1888. This was to catalogue all non-stellar objects [7]. William Herschel discovered NGC2371-2. He believed the two bright regions of this object were separate from one another and cataloged it as two separate objects. That is why NCC 2371 is also NGC 2372. In 1918 Heber D. Curtis found NGC 2371-2 to be a PN [5]. Since its discovery it has been studied by multiple groups due to its odd structure.

In 1978, the nebula was compared with the optical and radio structure. The study found a strong mass concentrate opposite of a decreased surface brightness [8]. Another study, done in 1981, searched for double envelopes in multiple planetary nebulae. The study found two symmetrical ansae or handles with the two bright lobes. This agreed

with previous work done by Perek and Kohoutek from 1967. No other additional structure was found in this study [9].

In 1982, a paper entitled "Spatial-Kinematical Models of Planetary Nebulae: NGC 2371-2." According to this paper, there are three separate structural regions in NGC 2371-2. The first is a central, oval ring which consists of two lobes. The second is an elliptical faint region of 75 x 50 arcsec. This region is best defined in the NW region of the nebula. The third region is a faint outlier, which is about 62 arcsec [10].

They found the central ring to have minimal eccentricity with the major axis at 65 arcsec and a minor axis of approximately 50 arcsec. The plane of the ring lies at about 25 degrees from the line of sight. The faint, elliptical region is an ellipsoid at three axes. The major axis makes an angle of about 65 degrees with the line of sight. This is essentially perpendicular to the central bright ring. The two other axes coincide with the axis of the central ring. The third outlier region lies approximately 62 arcsec from the central star. This region is suggested to be an ellipsoid at three axes [10]. NGC 2371-2 has a very complex structure and has been simplified into a basic model.

In 1988, the paper "The Evolution of Planetary Nebulae III. Position-Velocity Images of Butterfly-Type Nebulae" was published. The observations are considered in terms of a fast spherical wind. The paper suggests that much of the energy within the nebula is supplied by the wind. The velocity range of this object is at $\pm$ 36 km s^{-1} in the Hα emissions. The two bright knots were found to be displaced by $\pm 10 kms^{-1}$ with respect to the nebular velocity and the faint E and W regions were found to have a relative motion about two times the velocity of the bright knots [11].

There have been many studies on this object to better understanding of the structure. Previous work was done with shorter exposure time and with only four spectral positions in the case of Sabbadin et al. Because of the exposure limitation, the faint regions in this object were unknown. Currently, it is now easier to take longer exposures which allow the faint regions to appear.

II Thesis Statement

Previous research has had equipment limitations in studying this nebula. Using deep field images and making contour plots of these images further structure of the nebula can be found and compared to prior work.

III Method

3.1 Observations

The observations of NGC 2371-2 were made over a three night period in March 2008. The data was collected using the University of Arizona's Steward Observatory 61 inch Kuiper Telescope on Mount Bigelow. Images were taken with the Mont4K Charged Coupled Device (CCD). The CCD size is 4096 x 4097 pixels with an image scale of 0.14 arcsec/pixel. The field of view with this camera is 580 x 580 acrsec^2. The dark current on the chip is 16.5 electrons/pixel/hour and the camera's operating temperature is at -130 C.

Since the nebula emits the most light from doubly ionized oxygen, a narrow band [O III] filter centered at 5007 $\AA$ was used. Exposures were taken in five minute increments

for these three nights. The exposure time was based on the pointing accuracy of the telescope and atmospheric turbulence. Each night 36 exposures were taken giving a total of 108 exposures. There are several advantages of taking short exposures. In the event of a telescope malfunction or strong atmospheric turbulence, a short exposure may become distorted. If this were to happen, the problem could be realized with only a short amount of time wasted and only one frame that would be discarded. If a problem occurred with a longer exposure, more time would be wasted since the problem may have only occurred once over a long period of time. Another reason for shorter exposures is because the level of background noise increases as the exposure time increases. Throughout the observing run, the temperature, humidity, winds peed and cloud cover was checked every hour. This was to ensure proper observing conditions throughout the night.

3.2 Imaging

The PN NGC 2371-2 has a magnitude of 13. Short exposures of this object does not allow for much detail of the fainter parts of the nebula. The gas in a PN is dispersed and although it is very hot it does not glow very bright. This is the reason longer exposure time is necessary. Once the series of images have been stacked, image becomes much clearer and more detailed. This is because more light is being collected from a series then just one exposure. The same can be said about telescopes. The larger the mirror, the more light can be collected and the clearer the image. To compare the 61inch Kuiper to a 6 inch telescope, the light gathering power of the Kuiper telescope would be about 103 times more powerful.

Once all the images were collected for the night a series of darks, flats and biases were taken. Darks are images taken with the shutter of the CCD still closed. This is done to detect any thermal noise on the CCD chip for a specific time and temperature. Throughout the observing run the CCD Dewar was filled with liquid nitrogen. This is because the lower the camera temperature the less thermal noise is on the chip. The bias frames are taken at zero exposure time with the shutter closed. The noise produced in these frames is produced by the electrical components connected to the CCD chip. These frames detect any residual noise that is always present in the camera system, regardless of exposure time. Flat field frames are taken to account for variations in brightness, reflections and optical impurities, such as dust, within the optics system. Flat fields are taken by aiming the telescope at an evenly illuminated flat surface within the dome [12].

After the observing run, the images were calibrated. Calibrating allows for the best possible final image by reducing noise and defects in each frame. To reduce the data, master flats, darks and biases are made. To create a master dark each dark frame is subtracted by a bias frame. These frames are then averaged to create the master dark. A master flat is made by subtracting the bias frame from each flat. Then each of the flat minus bias frame is subtracted from the master dark frame. The dark frame must be same amount of exposure time as the flat. These frames are then averaged at 1. The image frame is then subtracted from the bias frame. This bias subtracted image frame is then subtracted by the master dark which once again must be accounted to the same exposure time. This frame is then divided by the master flat. This

is done for each image. Each calibrated image frame is then added to produce the final image. The same technique is done when using other filters; however, the flat field frames must have the filter in place for the flat fields to reduce the optical impurities caused by the filter.

Further observations of NGC 2371-2 were made in January 2009 over the course of one night. These observations also took place at University of Arizona's Steward Observatory 61 inch Kuiper Telescope on Mount Bigelow with the Mont4K CCD camera. However, images were taken with broadband filters, red (r), green (v) and blue (b). CCD cameras produce black and white images. To take a true color image of and object, three filters are needed, r, v and b. When imaging an object such as a planetary nebula, a 2 minute exposure taken with a green filter can appear to have more gas than a 2 minute exposure taken with a red filter. This is because PNe give off most of their light in the green end of the spectrum. Using the program MaxIm DL, a process can be taken called Combine Color. In this process the filtered images can be given a color within the program. The three calibrated images are then stacked to form a tricolor image.

The purpose of the tricolor image was to distinguish if anything can be detected within the structure of the nebula that was not detected with the [O III] filter. Although the majority of the nebula glows from the doubly ionized oxygen, it is still possible that more can be learned with a full color image since it is not composed of only [O III]. Referring back to Fig.2, strong emission lines can be seen in the red, from H_α and [N II], and blue from [N II] and [O II]. The exposure time for each filter was 2 minutes and the total exposure time for each filter was 1 hour.

When the three filtered images are combined the resulting image is not initially a true color image. This is due to the sensitivity of the chip within the CCD camera. The chip is more sensitive to red light than any other light. This results in am image that appears to be redder than what it actually is. This can be seen when the WD does not appear to be white in the image. To account for the color distortion, adjustments to the color can be made in MaxIm DL. For objects such as PNe, the WD can be used as a guide for color balancing, since the color of the star is known.

When the image is stacked, high intensity regions may be visible and low light areas may not be. To see both the high intensities and low intensities, a histogram is used to bring out both the dim and bright areas of the object. As seen in Fig. 4, this histogram is adjusted to a curved line. This brings down the intensity of the brighter parts of the nebula and brightens the fainter regions.

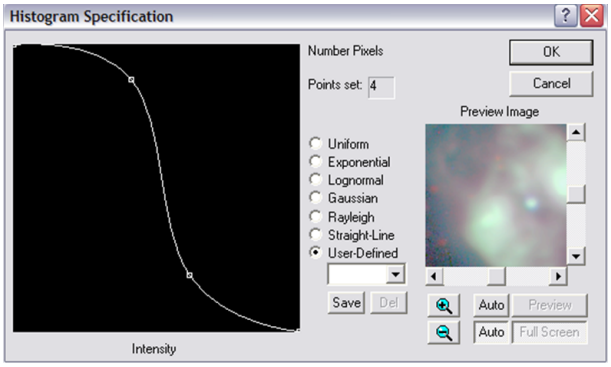

Figure 4: Histogram

3.3 Contouring with Iraf

For a basic idea of the structure, contour plots are made. This maps intensity levels that may not be picked up by the human eye. Regions of similar intensities in the planetary may be a result of the same evolutionary stage. Multiple contour plots were made, using Iraf, for a better understanding of the structure of the nebula. Iraf stands for Image Reduction and Analysis Facility. It is commonly used for data analysis of astronomical objects.

The contour plots show structure in the higher and lower intensities within the nebula. This is the first step in having an understanding of the structure. The contour plots are of the 9 hour [O III] image. There are 7 contour plots. The first six plots range between 40,000 and 70,000. Each plot has 10 contours with an interval of 5,000 counts. The final plot is the 6 plots stacked into one plot. These plots can be found in the Contours and Figures section in Figs 6- 12. With the contour plots a simplified structure can be found. This involves the basic shapes of nebulae such as cones, spheres, and rings.

IV Results and Discussion

The 108 [O III] frames were calibrated with the master dark and flat field frames. Each 108 frames had a total exposure time of 5 minutes. This gives a total exposure time of 9 hours. The resulting image can be found in Fig 5. The contour plots of this image can be found at the end of the paper in the Contours and Figures section.

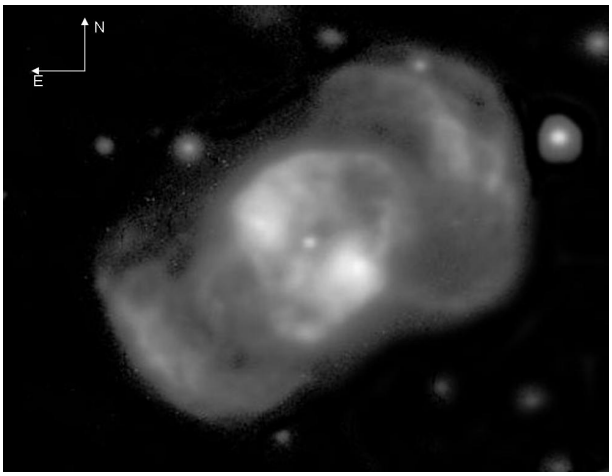

Figure 5: 9 Hour exposure of NGC 2371/2

The first contour plot in Fig. 6 has the lowest intensities within the nebula. This plot shows the outer most regions of the nebula are connected with the rest of the nebula. This also indicates how much further the gas extends than what was previously thought. It also shows an odd bubble in the SW end of the nebula. This bubble is not seen on the opposite end of the nebula indicating asymmetry. The following plots increase in intensity by 5,000 counts. These plots appear to agree with the previous research of Sabbadin et al. Each individual contour plot gives an indication of the evolution of the nebula along with an indication of the basic structure. In the final contour plot, in Fig. 12, all the contour plots are combined. In this, the brightest regions were noted to have asymmetry with the central star.

The r, b, and v filters were stacked separately before creating the final color image. All three images were adjusted with the same histogram specifications as in Fig. 4. In comparing the r, b, and v images, the b and v filtered images look fairly similar, as seen in Fig. 13 and Fig. 14. However, there still appears to be slightly more detail in the green filter. With the r filter image, there is clearly much less structure visible. This is not caused by exposure time or chip sensitivity within the CCD camera. The exposure time is the same, and the chip in the CCD is more sensitive to red light than green or blue. If NGC 2371-2 emitted white light, these images would look almost identical. The difference in the images indicates that the outer structure of the planetary has close to no red light, as seen in Fig. 15. In other words, the object glows more towards the green and blue end of the spectrum.

Although the red filtered image has less of the outer, dim, structure of the nebula, it still provides structural information near the WD. For the most part the structure around the WD looks very similar however; details can be resolved that could otherwise not be in the cases of the v and b filters. In the b, v, and [O III] images, it appears that the two brightest sections of the nebula are nothing more than bright knots or lobes in the nebula. This is most likely due to the fact that the nebula is giving off most of its light in those colors and therefore those two regions become blended in with the rest of the nebula. In the red image it appears that these are not just a bright but two jets of gas moving in opposite directions, as seen in Fig. 16. What was originally believed to be part of an off centered donut now appears to be two jets. The suggested jets do not lie along the line of sight. The NE jet appears to be moving away from Earth more so than the SW jet. The SW 'jet' appears to be moving towards the observer and SW and the NE jet appears to be moving NE and away from the observer. The NE jet has a position angle of approximately 60^o and the SW jet has a position angle of approximately -120^o.

Fig. 15 draws a line through the WD and across the nebula. It can be seen that the brightest regions do not line up with the central star. This may be due to the fact that one jet has less gas in front of the line of sight than the other. The brightest region of the jet further away from the observer may be skewed by the gas within the nebula.

The bubble in the SW end of the nebula, seen in both the [O III] image and the contour plot, may be part of a larger cone connecting the outer most shell of gas to the inner part of the nebula. If this is the case, the SE shell could have a similar cone structure that is not seen due to the orientation of the nebula.

The final stacked image of the r, v, and b filters can be seen in Fig. 17. This exposure time totals to three hours total. Fig. 16 was produced by bringing down the brightness levels of the lower intensities to observe the bright jets.

V Implications of Research

A basic understanding of the structure of NGC 2371/2 will help determine the direction of the gasses as they move away from the central core of the star. This information can be used for later work with a spectrograph which will provide the velocities of the gas. This information will ultimately determine the true structure of the nebula.

VI References

1. Arny,Thomas T. Explorations: An Introduction to Astronomy. 4 ed. New York: McGraw-Hill, 2006.

2. Kaler,James B. *Extreme Stars: At the Edge of Creation.* Cambridge: Cambridge University Press, 2001.

3. Shore, Steven N. Tapestry of Modern Astrophysics. Hoboken, N.J: Wiley-Interscience, 2003.

4. Carroll, Bradley W, and Dale A Ostlie. *An Introduction to Modern Astrophysics.* 2 ed. Adam R. S. Black. San Francisco: Addison-Wesley, 2007.

5. Hynes,Steven J. *Planetary Nebulae: A Practical Guide and Handbook for Amateur Astronomers.* Richmond: Willmann-Bell Inc., 1991.

6. Gurzadyan,Grigor A. *The Physics and Dynamics of Planetary Nebulae.* Immo Appenzeller, Rudolf Kippenhahn, Gerhard Borner, Peter A. Strittmatter, Martin Harwit, VirginiaTrimble. New York: Springer-Verlag, 1997.

7. Birney, D. Scott, Guillermo Gonzalez, and David Oesper. *Observational Astronomy.* 2 ed. Cambridge University Press, 2006.

8. Felli,M., M. Perinotto and "A Comparison of Optical and Radio Structures of Planetary Nebulae." *Astronomy and Astrophysics* 76, no. 69F (1979): 69-74.

9. Louise,R., F. Michel, and J.C. Mevolhon. "A Search for Nebulosities Associated with Planetary Nebulae." itshape Astronomy and Astrophysics 102, no. 303L (1981): 303-306.

10. Sabbadin,F., A. Bianchini, and E. Hamzaoglu. "Spatial-Kinematical Models for Planetary Nebulae: NGC 2371-2." *Astronomy Astrophysics*(1982): 523-528.

11. Icke,Vincent, Heather L. Preston, and Bruce Balick. "The Evolution of Planetary Nebulae III. Position-Velocity Images of Butterfly-Type Nebulae." *The Astronomical Journal* 97, no. 462I (1989): 462-625.

12. Stuart,Adam M. CCD *Astrophotography High-Quality Imaging from the Suburbs.*Practical Astronomy. New York: Springer Science + Business Media, Inc., 2006.

Contours and Figures

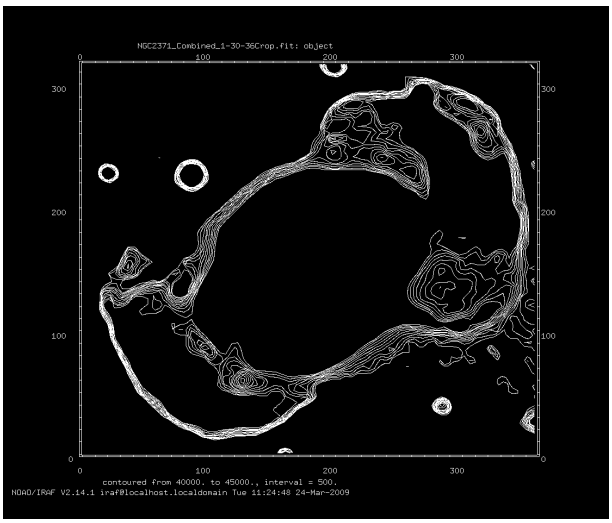

Figure 6: 40,000 - 45,000 counts

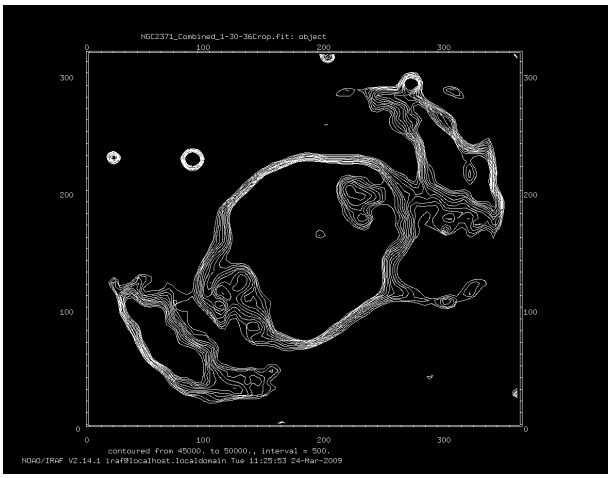

Figure 7: 45,000 - 50,000 counts

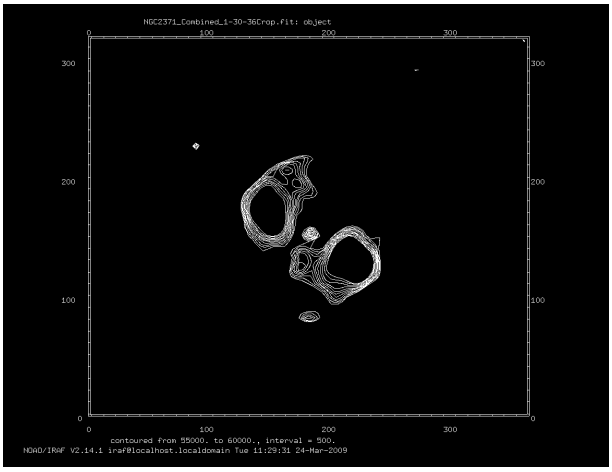

Figure 9: 55,000 - 60,000 counts

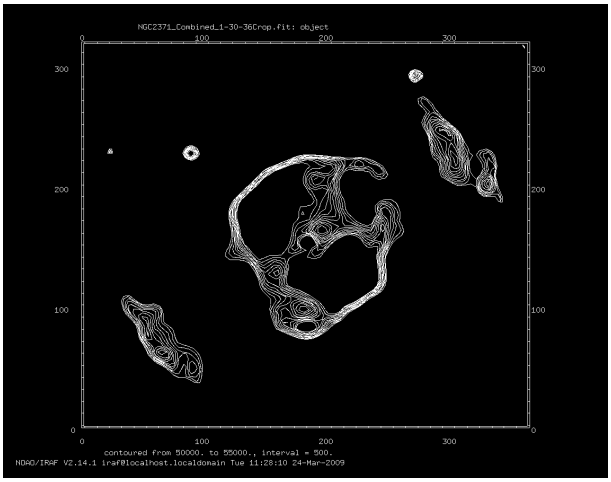

Figure 8: 50,000 - 55,000 counts

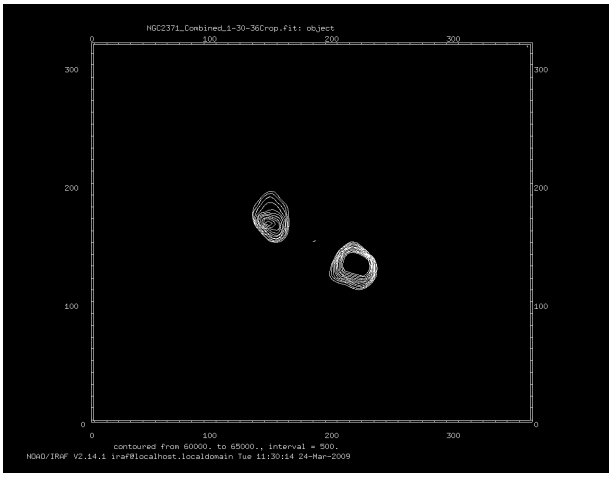

Figure 10: 60,000 - 65,000 counts

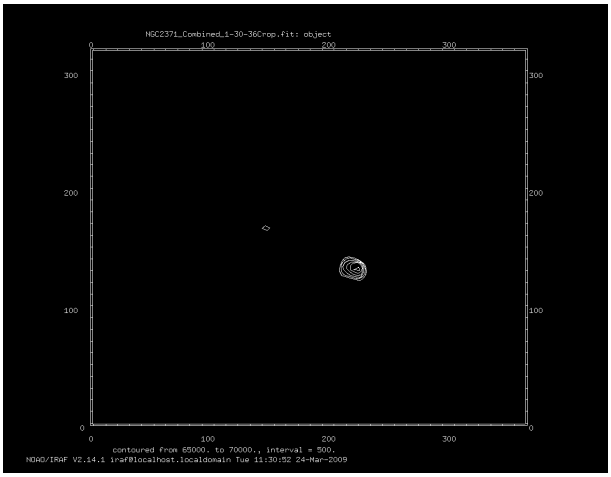

Figure 11: 65,000 - 70,000 counts

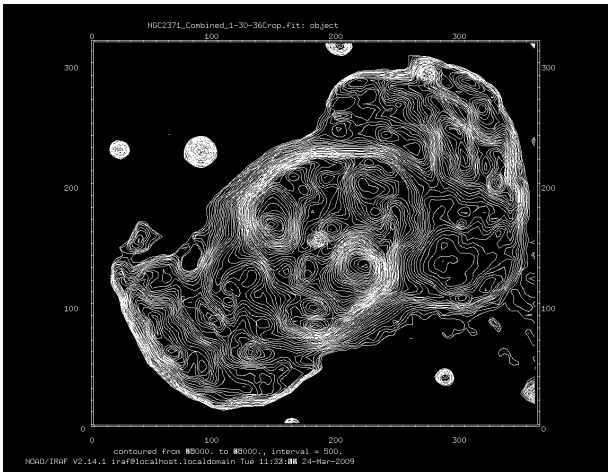

Figure 12: 40,000 - 70,000 counts

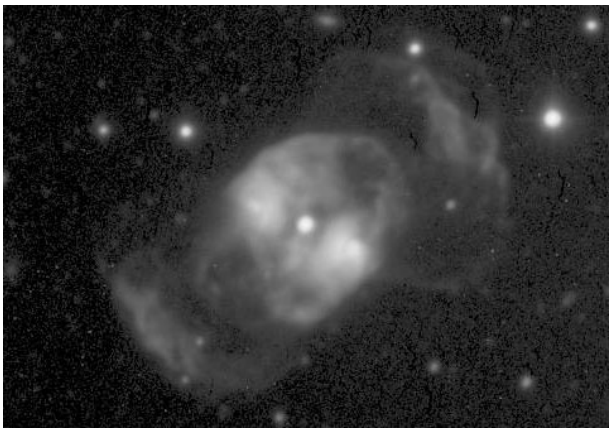

Figure 13: 1 Hour Exposure with Blue (B) Filter

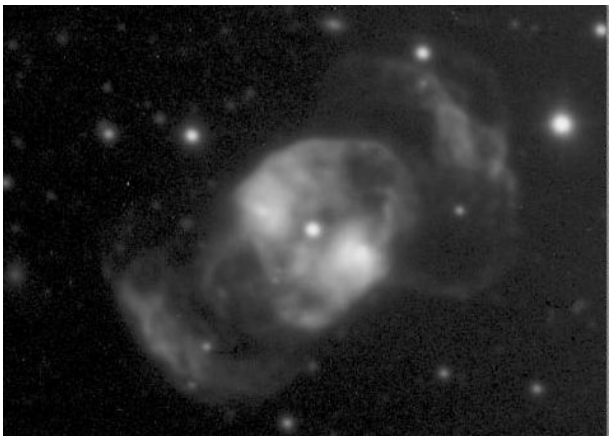

Figure 14: 1 Hour Exposure with Green (V) Filter

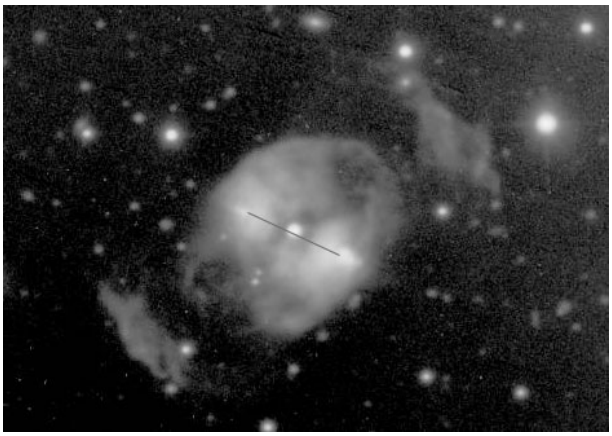

Figure 15: 1 Hour Exposure with Red Filter

Figure 16: 3 Hour Tri-Color Exposure of NGC 2371/2

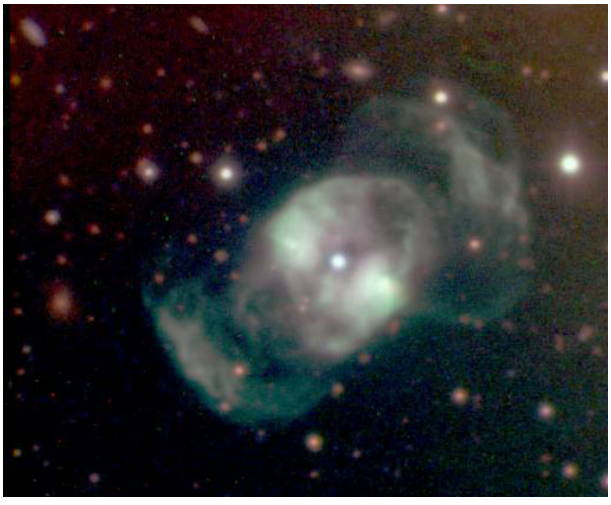

Figure 17: 3 Hour Exposure with R, V, and B Filters